

The influence of deviation in the centroid and entry angle of the bullet on its motion inside the barrel

Xiaoyun Zhang^{a*} , Cheng Xu^b 

^aEngineering Technology Training Center, Nanjing Vocational University of Industry Technology, Nanjing 210023, China. E-mail: xyzhang531@163.com

^bSchool of Mechanical Engineering, Nanjing University of Science and Technology, Nanjing 210094, China. E-mail: xucheng62@mail.njust.edu.cn

*Corresponding author

<https://doi.org/10.1590/1679-78258060>

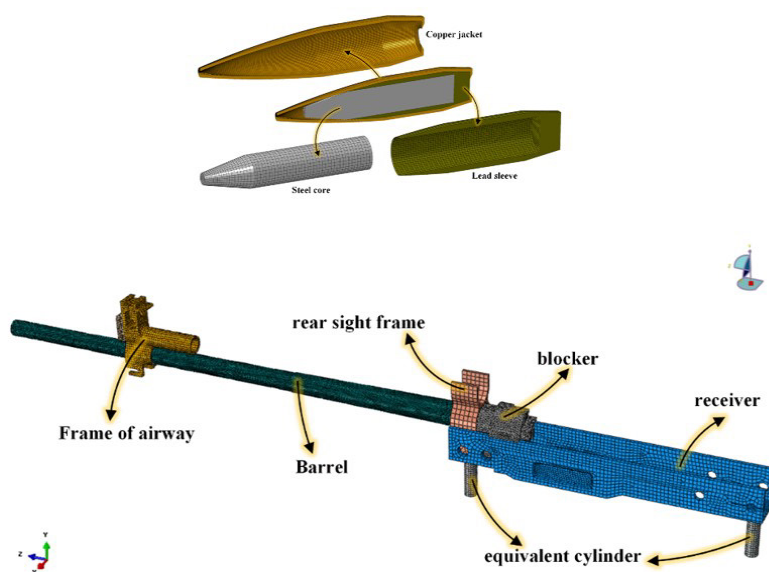
Abstract

The characteristics of a bullet are closely related to its shooting accuracy. In actual shooting, the centroid and entry angle of the bullet always deviate from the ideal state. To study the influence of these two parameters on the movement of the bullet, a finite element model of the bullet movement inside the barrel was built based on a 5.8 mm small-caliber rifle to simulate the actual process of firing bullets. In this model, the pressure load of the real gunpowder gas on the bullet was considered. This model was also verified by experiments and the relative error is less than 1.5%. The result shows that the influence the centroid and entry angle of the bullet are mainly reflected in the amplitude and phase angle of the bullet swing angle. The larger the offsetting distance of centroid is, the amplitude of the pitch and yaw angle are. The maximum magnitude of amplitude is 0.2° . The difference of swing angle in phase is equal to the difference in offsetting angle. The curve characteristics of different deviation angle are similar to the curve of bullet centroid effect. The range of the pitch angle is $-1^\circ \sim 0.9^\circ$ and the range of the yaw angle is $-0.9^\circ \sim 0.9^\circ$.

Keywords

shooting accuracy, bullet centroid, entry angle, finite element, bullet motion inside the barrel

Graphical Abstract



Received: February. 23, 2024. In revised form: July 11, 2024. Accepted: August 04, 2024. Available online: August 08, 2024.

<https://doi.org/10.1590/1679-78258060>



Latin American Journal of Solids and Structures. ISSN 1679-7825. Copyright © 2024. This is an Open Access article distributed under the terms of the [Creative Commons Attribution License](https://creativecommons.org/licenses/by/4.0/), which permits unrestricted use, distribution, and reproduction in any medium, provided the original work is properly cited.

1 INTRODUCTION

The movement process of bullets inside the barrel is an important part of the research on shooting accuracy. Many scholars have studied the impact of this movement process on shooting accuracy from the perspective of simulation.

In terms of theoretical research, the initial projectile/gun interaction model was committed to construct a simplified model of gun vibration under the action of projectile excitation. Many scholars have adopted the Bernoulli-Euler beam theoretical model (Hua et al., 2017). Barari et al. (2011) explored the nonlinear vibration behavior of Bernoulli-Euler beams under axial loading. Kumar P et al. (2014) used an analytical method to analyze the vibration model of the barrel. Ning and Yang (2010, 2012) simplified the barrel into an equal-section cantilever beam, established the barrel vibration equation according to the Bernoulli-Euler primary beam theory, and solved the barrel vibration equation by modal analysis. Mu (2002) and Jiang and Guo (2002) studied the vibration problem caused by the accelerated motion of a projectile in the barrel. The barrel was simplified as a cantilever beam and the action of the projectile was simplified as an accelerating load. They established the motion equation of the barrel and obtained an analytical solution in series form. In the study of Ismail Esen and Koç (2015a), the dynamic interaction between a 120 mm smoothbore tank barrel modeled as an Euler-Bernoulli cantilever beam and an accelerating projectile during firing is presented. Ismail Esen and Koç (2015b) also presented a new method that determines the non-linear behavior of the barrel with a passive vibration absorber and optimizes the absorber using the genetic algorithm (GA). Ding and Xie (1999) simultaneously considered the effects of projectile gravity, static deflection, and dynamic deflection on the vibration of the gun barrel in the model, when studying the lateral vibration of the gun barrel caused by the motion of a projectile in the bore. They obtained a general solution for the entire process of gun barrel vibration during a single shot using the perturbation method. Hua et al. (2018) and Hua (2019) simplified several typical dynamic elements during machine gun firing into two types of elastic beam dynamic problems: eccentric rotating beam and axially moving cantilever beam. They studied their dynamic problems and proposed an efficient dynamic analysis method suitable for axially moving cantilever beam problems.

In terms of simulation models, many scholars have conducted research on barrel vibration and the interaction between bullets and guns in small-caliber firearms. Leonhardt and Garnich (2019), Vitek R(2008,2009), Moldoveanu C et al. (2010), Sava A C et al. (2015) and S Deng et al. (2014) studied the effects of barrel models and boundary conditions on simulation, comparing the changes in muzzle displacement of different barrel models, and considering both temporal and spatial variations in the application of chamber pressure. Ismail Esen(2011) developed a MATLAB code for numerical solutions. The accelerating moving mass that is travelling on the beam was modelled as a moving finite element in order to include inertial effects beside gravitation force of mass. Bernd D et al. (2019) separated the regular and random motion of the bullet in the bore based on the simulation model and estimated the shooting accuracy by the deviation of the random motion. Fan and He (2011) used a dynamic display algorithm and grid adaptive technology to study the extrusion process of lead bullet through numerical simulation and analyzed the formation process of rifling marks on the bullet and the material flow situation. However, this calculation model simplified the barrel as a rigid surface and did not consider the flexibility of the barrel. Qi Xin et al. (2013) used the finite element method to analyze and compare the natural frequencies of the conical barrel, the cylindrical barrel and the twist barrel. Koç Mehmet Akif et al. (2016) proposed a new method that combines a precise Finite Element Method(FEM) with Artificial Intelligence(ANN), and can be used for determining the exact dynamic behaviour of a barrel for some cases and then for precisely predicting the behaviour for all other possible cases of firing. Yang et al. (2020a) established a thermal coupled finite element model of a small caliber rifle and introduced a friction subroutine to study the action process inside the bore. In the above studies, in order to save computational time, the barrel model of the bullet/barrel interaction is mostly a simple barrel that does not consider other components, ignoring the effects of the entire gun system. The application of barrel constraints and loads may differ from the actual situation. Shuli Li et al. (2023) simulated the barrel chamber mechanical wear model in the whole life cycle by using the ALE mesh adaptive technology. Bui and Nguyen (2023) study the effects of rifling parameters such as the quantity of grooves n , groove width a , depth of groove t , radius of groove corner ρ by using Ansys software.

It is also difficult to observe the motion of bullets during the process of bullet/gun interaction in experiments. Using the finite element numerical simulation method makes it easier to observe the motion law of the bullet in the gun. In this paper, the influence of centroid offsetting distance, centroid offsetting angle, and entry angle of bullet was studied by finite element method. A finite element model of the bullet movement inside the barrel was built based on a 5.8 mm small-caliber rifle to simulate the actual process of firing bullets. In this model, the pressure load of the real gunpowder gas on the bullet was considered.

2 ESTABLISHMENT OF THE MODEL

2.1 Finite element (FE) model

(1) FE model of bullet

The FE model of 5.8 mm rifle bullet is shown in Figure 1. Based on the actual geometry, the bullet is composed of copper jacket, lead sleeve and steel core. The most FE elements of bullet are eight-node linear hexahedron element (C3D8R). The calculation time of this kind of mesh in the bullet movement inside the barrel model is shorter and the calculation accuracy is better. The number of elements is shown in Table 1. Considering the deformation of copper jacket is sharp in the process of the bullet movement inside the barrel, the mesh of jacket was built to have a higher element density than lead sleeve and steel core.

Table 1 The number of bullet and gun elements

Bullet	Copper jacket		Lead sleeve			Steel core
Number of elements	58560		8520			5706
Gun	barrel	frame of airway	rear sight frame	blocker	receiver	equivalent cylinder
Number of elements	177102	40718	3282	13521	30642	1280

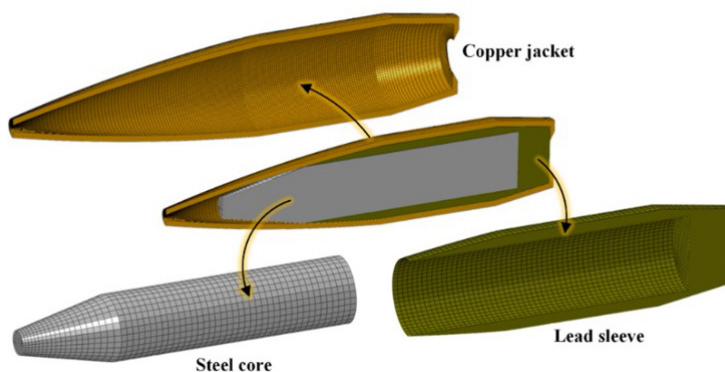


Figure 1 FE model of bullet

(2) FE model of gun system

The FE model of the gun is shown in Figure 2. In addition to the barrel, it also includes a simplified frame of airway, rear sight frame, blocker and receiver. Two equivalent cylinders are added under the receiver. By adjusting the material density and position of the cylinder, the mass and center of gravity of the whole model can be close to the whole gun model. The most FE elements of the barrel are eight-node linear hexahedron elements (C3D8R). The FE elements of the receiver, rear sight frame and two equivalent cylinders are mainly hexahedron elements. The shape of the frame of the airway and blocker is complex. To ensure the quality of FE elements, tetrahedral element is mainly used. Considering the load and constraint factors, the mesh of the barrel, frame of airway, blocker and receiver are denser than other parts. The number of meshes of each part of the gun model is shown in Table 1.

The selection of mesh type and density for the model will have an impact on numerical calculations. The mesh type and density in this paper were based on the research of Yang et al. (2020b).

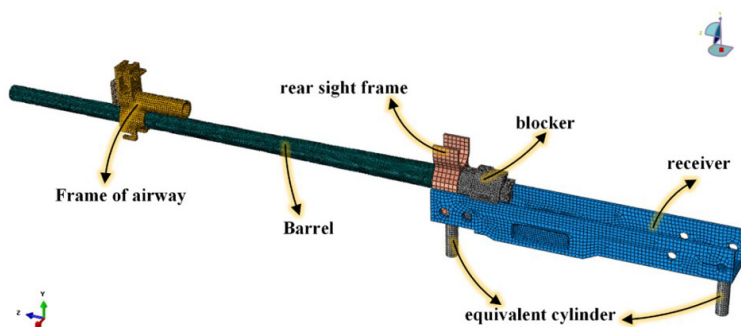


Figure 2 FE model of gun system

2.2 Material model

Under the pressure of gunpowder gas, the bullet will be squeezed and move along the rifling in a short time. Both copper jacket and lead sleeve are elastoplastic materials. In this process, the deformation of the bullet is serious, so it is necessary to adopt a suitable material model.

The Johnson-Cook(JC) constitutive model was usually applied to the copper jacket in the numerical simulation. The JC model represents an empirical relationship for the von Mises flow stress. This model was first proposed in 1983 with the following standard form (Johnson and Cook, 1983):

$$\sigma = (A + B\varepsilon^n)(1 + C \ln \dot{\varepsilon}^*)(1 + T^{*m}) \tag{1}$$

where σ is flow stress, ε is the equivalent plastic strain, $\dot{\varepsilon}^* = \dot{\varepsilon} / \dot{\varepsilon}_0$ is the dimensionless plastic strain rate for $\dot{\varepsilon}_0 = 1.0 / s$ and T^* is the homologous temperature. The constants are A, B, C, n and m. The expression in the first set of brackets gives the stress as a function of the strain for $\dot{\varepsilon}_0 = 1.0 / s$ and $T^* = 0$. The expressions in the second and third sets of brackets represent the effects of strain rate and temperature, respectively.

The copper material parameters of JC model are shown in Table 2.

Table 2 The copper material parameters of the JC model

A(MPa)	B(MPa)	n	C	m
90	292	0.31	0.25	1.09

The Cowper-Symonds is a typical material model used to describe the mechanical behavior of lead at a high strain rate. The dynamic effects of strain rates are considered by scaling the static yield stress. This model is expressed as (Zhang et al.,2019):

$$\frac{\sigma_d}{\sigma_0} = 1 + \left(\frac{\dot{\varepsilon}}{D}\right)^{1/P} \tag{2}$$

where σ_d is the dynamic yield stress, σ_0 is the static yield stress, and D and P are constants. However, the C-S model only focuses on the change of yield strength with strain rate and ignores other stress-strain points on the stress-strain curve under various strain rates. Some scholars have adopted a generalized Cowper-Symonds model. This model is expressed as (Zhang et al.,2019)

$$\frac{\sigma}{\sigma_s} = 1 + \left(\frac{\dot{\varepsilon}}{D}\right)^{1/P} \tag{3}$$

where σ_s is the static stress (variable with time), and the other parameters and constant definitions are the same as those of the original Cowper-Symonds material model. The modified C-S constitutive equation of lead can be expressed as $\sigma / \sigma_s = 1 + (\dot{\varepsilon} / 11359)^{1/10.469}$.

Other basic material properties of bullets are shown in Table 3.

Table 3 Basic material properties of the bullet andgun

Part	Density (kg/m ³)	Young's modulus (MPa)	Poisson ratio	
Bullet	Steel core	7.85×10 ³	206000	0.29
	Copper jacket	8.73×10 ³	108000	0.35
	Lead sleeve	11.34×10 ³	17000	0.42
Gun	barrel	7.85×10 ³	210000	0.3
	receiver	2.7×10 ³	72000	0.3
	frame of airway, rear	7.8×10 ³	17000	0.3
	sight frame and blocker			

The barrel is made of 30SiMn₂MoVA steel. The frame of airway, rear sight frame and blocker are made of high-strength steel. The receiver is made of aluminum alloy. The material parameters of the gun are show in Table 3.

2.3 Contact and restraint

The steel core, lead sleeve and copper jacket were tied each other to ensure there was no sliding between them. The parts of gun were also tied to each other. Using Surface-to-Surface contact type to define the contact between the outer surface of the bullet and the inner bore of the gun barrel. The contact state starts to work from the initial step.

The restraint position of the gun is shown in Figure 3. The restraint mode is the same as the experimental gun. The displacement of the corresponding node on the receiver in three directions is limited.

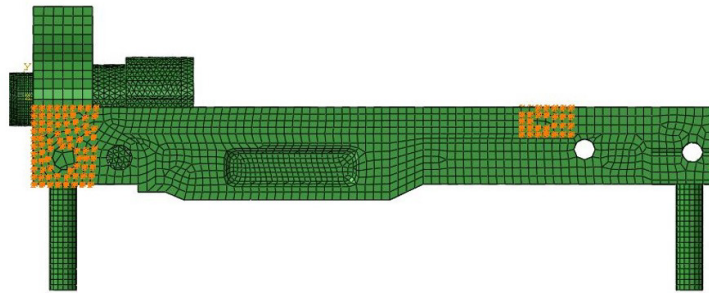


Figure 3 The restraint position of the gun

2.4 Pressure boundary conditions

In the typical numerical simulations of bullet/gun interactions, only the effect of gas pressure applied to the bottom of the bullet is considered. The effects of the pressure on bottom of bullet, the pressure on bottom of gun and the pressure in the airway were considered in the present work.

Pressure development assessment is shown in Figure 4, where P is the average pressure of 5.8 mm small-caliber rifle, P_t is the bottom pressure of the gun, P_s is the pressure in the airway. P_t was calculated by P , and P_s was calculated by P_t . The peak time of the P_t curve is close to that of P . The peak time of the P_s curve is later than P curve due to the movement of bullet.

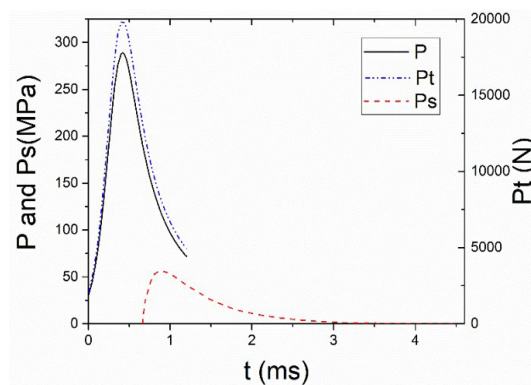


Figure 4 Time history of the pressure in the gun

The average pressure curve load directly in the form of time onto the bottom and tail cone of the bullet. This application method is simple to implement and requires less time to calculate.

The Lagrangian assumption of classical interior ballistics ignores the influence of the recoil of the gun. The bottom pressure of the gun P_t along the axis is not taken into account. The calculation method of P_t is:

$$P_t = \frac{\pi}{4} d_1^2 P \tag{4}$$

where d_1 is the inner diameter of the bottom of the bullet.

For gas-conducting weapons, the pressure in the gas airway also has a significant impact on barrel vibration. The variation law of propellant gas pressure in the airway is related to the variation law of pressure in the gun. The pressure in the airway P_s can be calculated as:

$$P_s = P_d e^{-\frac{t_s}{b}} (1 - e^{-a \frac{t_s}{b}}) \quad (5)$$

where t_s is the time calculated from the moment the bullet passes through the airway hole, b is the time coefficient related to the pressure impulse in the gun and $b = i_0 / P_d$, i_0 is the total impulse of the pressure of gunpowder in the gun, a is the structural coefficient related to the structural parameters of the airway device and $a = 1 / (1 / \eta_s - 1)$, η_s is the impulse efficiency of the airway device. Time history of pressure in the airway is shown in Figure 4.

2.5 Simulations performed

The movement of a bullet inside a barrel is a typical nonlinear dynamic problem. Explicit algorithms are suitable for solving complex nonlinear processes such as transient impacts, and can be used to handle the calculation of initial bullet insertion and bore motion processes. In this paper, ABAQUS was used to simulate the dynamic response of bullet launch process. And the simulations were completed by using Lenovo ThinkStation P710 workstation.

3 MODEL VERIFICATION

3.1 Experiments facilities

To verify the results of FE model, the shooting test of a typical 5.8 mm rifle has been done. The experiments were carried out in the indoor proving ground. The room temperature was 25-30°C. The experiment facilities are shown in Figure 5. The test gun was fixed on the special fixture. The speed of the bullet was measured by a double base optical speed detector which is 1.5 m away from the muzzle. The test result can be shown in the screen of speed detector directly.



Figure 5 The experiment facilities

3.2 Comparison of simulated results and experimental results

Ten groups of muzzle velocities were tested by groups of one shot. The results of experiments ranged from 911 to 912.9 m/s. The average muzzle velocity was 912.17 m/s (The 95% confidence interval is 911.84~912.50).

The velocity change of the bullet in numerical simulation is shown in Figure 6. The muzzle velocity is 926 m/s. The relative error between the simulation and experiment result is 1.5%. This indicates that the model established effectively represented the structure.

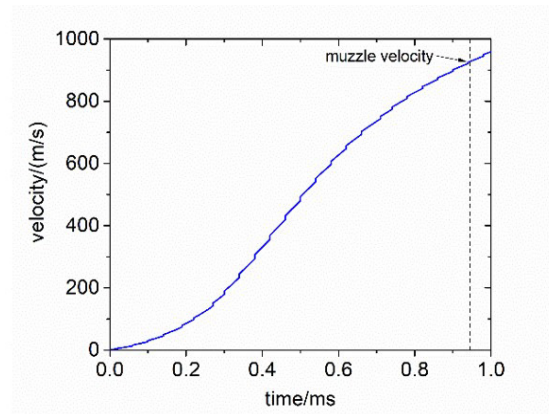


Figure 6 The velocity change of the bullet in numerical simulation

4 THE INFLUENCE OF DEVIATION OF THE BULLET PARAMETERS

4.1 The effect of centroid on the motion of bullet

Most researchers have assumed that bullets are symmetrical. However, during the actual production and assembly of bullets, mass eccentricity cannot be ignored. The characteristic parameters of mass eccentricity are shown in Figure 7 including: R_{CM} and α_{CM} . Point O is the ideal center of mass position, located on the rotating axis of the bullet. The X and Y axes pass through the O point and are perpendicular to the rotating axis of the bullet. Point CM is the actual center of mass position. R_{CM} is the offsetting distance between Point O and Point CM, and α_{CM} is the offsetting angle between the Point CM and the Y-axis.

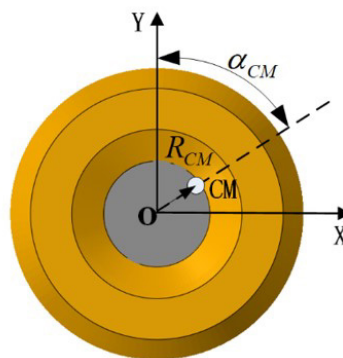


Figure 7 Schematic diagram of R_{CM} and α_{CM} .

4.1.1 The effect of offsetting distance R_{CM}

The effect of offsetting distance is shown in Figure 8(a) and Figure 9(a). The pitch and yaw angles of the bullet in the gun will be affected. Z is the distance the bullet moves in the bore. R_{CM} is 0 mm, 0.01 mm and 0.02 mm respectively which α_{CM} is 0° . As shown in Figure 8 (a), the pitch angle of the bullet will tilt downwards during the process in the gun. The moment when the maximum value occurs corresponds to the peak of the pressure in the air chamber. As shown in Figure 9(a), the yaw angle of the bullet changes regularly during the process in the gun. When R_{CM} is 0.01 mm, the pitch angle of the bullet increases significantly compared with the situation $R_{CM} = 0$, and the range of yaw angle is $-0.02^\circ \sim 0.02^\circ$. When R_{CM} is 0.02 mm, the amplitude of the pitch angle continues to increase, and the maximum magnitude is 0.2° , and the range of yaw angle is $-0.04^\circ \sim 0.04^\circ$. Compared with the situation $R_{CM} = 0$, the increase of offsetting distance will significantly increase the pitch and yaw angle in the bore. And the larger the offsetting distance is, the amplitude of pitch and yaw angle are.

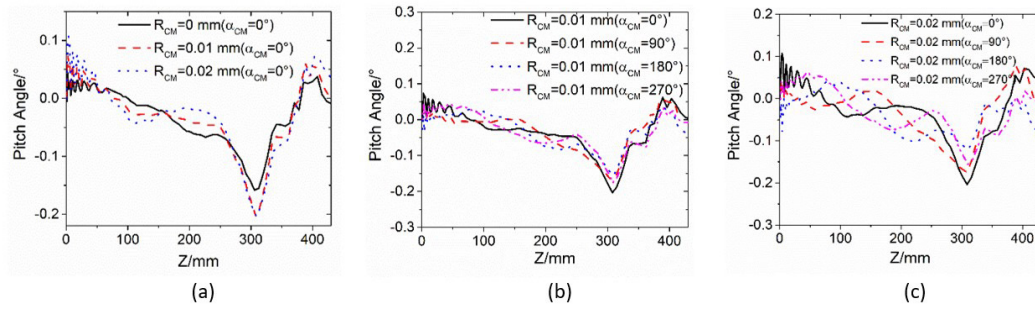


Figure 8 Pitch angle of bullet

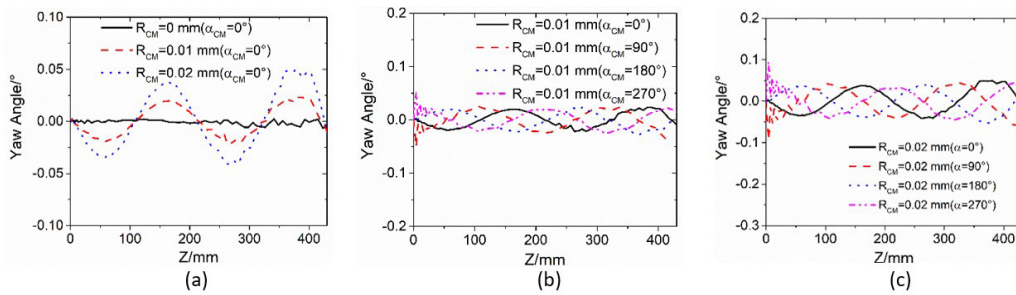


Figure 9 Yaw angle of bullet

4.1.2 The effect of offsetting angle α_{CM}

The effects of offsetting angle α_{CM} ($R_{CM} = 0.01 \text{ mm}$) are shown in Figure 8(b) and Figure 9(b). The amplitude of pitch and yaw angle of the bullet in the gun is not influenced by α_{CM} ($R_{CM} = 0.01 \text{ mm}$), but there is a difference in the curves of offsetting angle. The difference in phase is equal to the difference in offsetting angle. As shown in Figure 8(b), when α_{CM} is 0° and 180° , the pitch angle of the bullet fluctuates sharply during bullet engraving progress. Then the curve of pitch angle tends to change steadily. As shown in Figure 9(b), when α_{CM} is 90° and 270° , the yaw angle of the bullet also fluctuates sharply during bullet engraving progress. It can be seen that the offsetting direction will cause the movement of bullet in this direction to be unstable. The amplitude of pitch and yaw angle reach 0.05° during bullet engraving progress.

The effects of offsetting angle α_{CM} ($R_{CM} = 0.02 \text{ mm}$) are shown Figure 8(c) and Figure 9(c). The curve characteristics are the same as $R_{CM} = 0.01 \text{ mm}$. As shown in Figure 8(c), when α_{CM} is 0° and 180° , the pitch angle of the bullet fluctuates sharply during the bullet engraving progress. As shown in Figure 9(c), when α_{CM} is 90° and 270° , the yaw angle of the bullet also fluctuates sharply during the bullet engraving progress. The amplitude of pitch and yaw angle reach 0.1° during bullet engraving progress.

4.2 The effect of entry angle on the motion of bullet

In addition to the mass eccentricity during the manufacturing and production process, there is a deviation angle error of the bullet in the barrel during the loading stage caused by assembly and positioning. And the direction of the deviation angle is also random. The characteristic parameters of deviation angle are shown in Figure 10, which includes: α and β . β is the angle between the actual axis CL' and the ideal axis CL of the bullet. Point C is the centroid of the bullet. The Y_C and X_C axes pass through the C point and are perpendicular to the ideal axis CL of the bullet. α is the offsetting angle between the Point L'' and the Y_C axis, which L'' is the projection of L' in the plane $Y_C C X_C$.

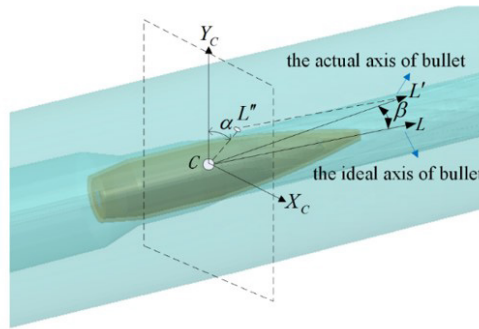


Figure 10 Schematic diagram of α and β .

4.2.1 The effect of deviation angle β

The effects of the deviation angle β ($\alpha = 0^\circ$) are shown in Figure 11(a) and Figure 12(a). When $\beta = 0.5^\circ$, the range of pitch angle is $-0.5^\circ \sim 0.4^\circ$ and the range of yaw angle is $-0.4^\circ \sim 0.4^\circ$. When $\beta = 1^\circ$, the range of pitch angle is $-1^\circ \sim 0.9^\circ$ and the range of yaw angle is $-0.9^\circ \sim 0.9^\circ$. Compared with the situation $\beta = 0^\circ$, the increase of deviation angle will significantly increase the pitch and yaw angle in the bore. And the larger the deviation angle β is, the amplitude of the pitch and yaw angle are.

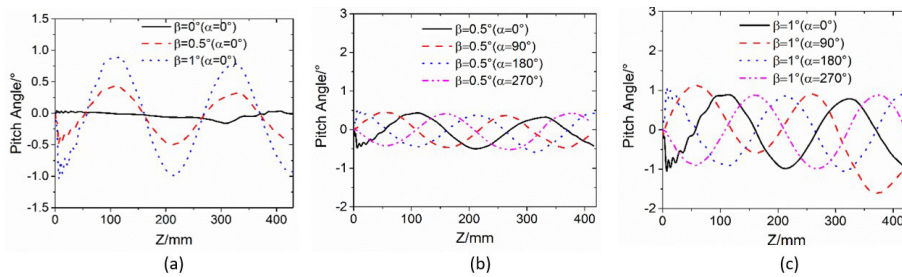


Figure 11 Pitch angle of bullet

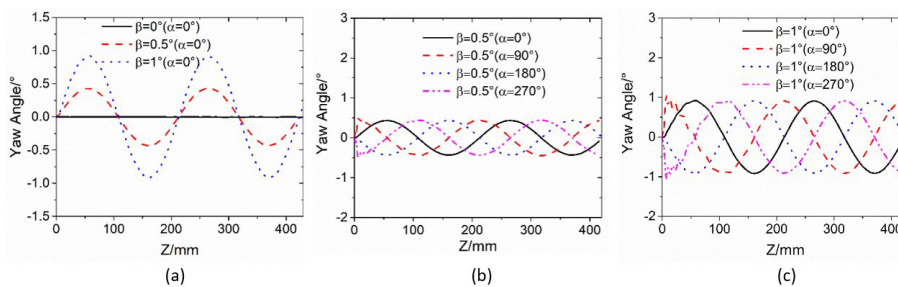


Figure 12 Yaw angle of bullet

4.2.2 The effect of deviation angle α

The effects of the deviation angle α ($\beta = 0.5^\circ$) are shown in Figure 11(b) and Figure 12(b). The amplitude of pitch and yaw angle of the bullet in the gun are not influenced by α and the range is $-0.5^\circ \sim 0.5^\circ$. But there is a difference in the curves of different angle α . The phase difference is equal to the difference in angle α . Similar to the variation pattern caused by offsetting angle α_{CM} , as shown in Figure 11(b), when α is 0° and 180° , the pitch angle of the bullet fluctuates sharply during bullet engraving progress. Then the curve of pitch angle tends to change steadily. As shown in Figure 12(b), when α is 90° and 270° , the yaw angle of bullet also fluctuates sharply during bullet engraving progress.

The effects of the deviation angle α ($\beta = 1^\circ$) are shown Figure 11(c) and Figure 12(c). The curve characteristics are similar to the curve when the angle $\beta = 0.5^\circ$. The range of pitch and yaw angle of the bullet in the gun is $-1^\circ \sim 1^\circ$.

5 CONCLUSIONS

The deviation of the bullet parameters has a great influence on the motion of the bullet in the gun. It mainly reflected in the amplitude and phase angle of the bullet swing. The influence of the deviation parameters on the bullet motion in a gun was compared and analyzed by the finite element simulation method. Based on the simulation results, some conclusions can be drawn as follows:

- (1) The effect of centroid offsetting distance was compared, when R_{CM} is 0 mm, 0.01 mm and 0.02 mm respectively which α_{CM} is 0° . The larger the offsetting distance is, the amplitude of the pitch and yaw angle are. When R_{CM} is 0.02 mm, the amplitude of the pitch angle continues to increase, and the maximum magnitude is 0.2° , and the range of yaw angle is $-0.04^\circ \sim 0.04^\circ$.
- (2) The effect of centroid offsetting angle α_{CM} was compared, when α_{CM} is 0° , 90° , 180° and 270° respectively which is R_{CM} 0.01 mm and 0.02 mm. The amplitude of the pitch and yaw angle of the bullet in a gun is not influenced by α_{CM} , but there is a difference in the curves of offsetting angle. The difference in phase is equal to the difference in offsetting angle.
- (3) The effect of the deviation angle α and β which related to entry angle was study. And the larger the deviation angle β is, the amplitude of pitch and yaw angle are. When $\beta = 1^\circ$, The range of the pitch angle is $-1^\circ \sim 0.9^\circ$ and the range of the yaw angle is $-0.9^\circ \sim 0.9^\circ$. The curve characteristics of different deviation angle α are similar to the curve of α_{CM} .
- (4) From the above results, it can be concluded that the centroid offsetting distance and the angle of entry into the deviation angle β have a significant impact on the amplitude of the bullet's oscillation during the period of bullet in barrel. These parameters will also have an impact on the dispersion range of the bullet on the target.

Acknowledgements

The authors would like to acknowledge the funding from the Start-up Fund for New Talented Researchers of Nanjing Vocational University of Industry Technology (Grant No. YK23-14-02).

Author's Contributions: Conceptualization, Xiaoyun Zhang and Cheng Xu; Writing - original draft, Xiaoyun Zhang; Writing - review & editing, Xiaoyun Zhang.

Editor: Marcílio Alves

References

- Barari A, Kaliji H D, Ghadami M, et al(2011). Non-linear vibration of Euler-Bernoulli beams. *Lat Am J Solids Stru* 8(2):139-148.
- Bernd D, Martin H and Axel S(2019). A numerical analysis of the in-bore motion small caliber projectiles. 31st International Symposium on Ballistics 1027-1039.
- Bui, V. Q., & Nguyen, T. V. (2023). Studying the Effect of Rifling Parameters on the Stress State in a Gun Barrel Wall When Firing. *Engineering And Technology Journal*, 8(8), 2556–2564.
- Fan Lixia, He Xiangyue(2011). Finite Element Simulation and Process Analysis of Projectile Entering into Barrel. *Acta Armamentarii* 32(8):963-969. (in Chinese)
- G.R. Johnson and W.H. Cook(1983). A Constitutive Model and Data for Metals Subjected to Large Strains, High Strain-Rates and High Temperatures, *Proceedings of the Seventh International Symposium on Ballistics* 541–547.
- Hua H, Liao Z, Zhang X(2018). The self-excited vibrations of an axially retracting cantilever beam using the Galerkin method with fitted polynomial basis functions. *J Mech Sci Technol* 32(1):29-36.
- Hua H, Qiu M, Liao Z(2017). Dynamic analysis of an axially moving beam subject to inner pressure using finite element method. *J Mech Sci Technol* 31(6):2663-2670.

- Hua Hongliang(2019). Study on the Dynamics of Eccentrically Rotating Beam and Axially Moving Cantilever Beam. Nanjing: Nanjing University of Science and Technology,China.
- Ismail Esen (2011). Dynamic response of a beam due to an accelerating moving mass using moving finite element approximation. *Mathematical & Computational Applications*, 16(1), 171.
- Ismail Esen, Mehmet Akif Koç (2015a). Dynamic response of a 120 mm smoothbore tank barrel during horizontal and inclined firing positions. *Latin American Journal of Solids & Structures*,12:1462-1486.
- Ismail Esen, Mehmet Akif Koç (2015b). Optimization of a passive vibration absorber for a barrel using the genetic algorithm. *Expert Systems with Applications*, 42(2), 894-905.
- Jiang Mu (2002).The dynamic response of a beam under a moving mass. *Mechanics in Engineering* 24(6):44-47. (in Chinese)
- Jiang Mu, Guo Xifu (2002). On the vibration of tube due to accelerately moving projectile. *Journal of Ballistics* 14(3):57-62. (in Chinese)
- Koç Mehmet Akif, Esen İsmail, Çay Yusuf (2016). Tip deflection determination of a barrel for the effect of an accelerating projectile before firing using finite element and artificial neural network combined algorithm. *Latin American Journal of Solids & Structures*, 13(10), 1968-1995.
- Kumar P, Nayak S K, Datar A M, et al. (2014). Analysis of transverse vibration modes of a gun barrel subjected to recoil. *Applied Mechanics & Materials* 592-594:2011-2015.
- Leonhardt D, Garnich M (2019). A finite element model to predict the influence of asymmetries on barrel dynamics in small arms. 31st International Symposium on Ballistics 1015-1026.
- Li Shuli, Wang Liqun, Yang Guolai (2023). Numerical calculation of barrel chamber mechanical wear based on the principle of dynamic pressure lubrication. *Journal of Physics: Conference Series*. 2478. 092010.
- Liu Ning, Yang Guolai (2010). Effect of Lateral Impact Between Projectile and Barrel on Dynamic Response of Tube. *Journal of Ballistics* 22(2):67-70. (in Chinese)
- Liu Ning, Yang Guolai (2012). Vibration property analysis of axially moving cantilever beam considering the effect of moving mass, *Journal of Vibration and Shock* 31(3):102-105. (in Chinese)
- Moldoveanu C, Somoiaig P, Tudor V, et al (2010). Research concerning the oscillations of the weapons systems barrels. *International Conference the Knowledge-based Organization*.
- Qi Xin, Shen Wenjie, He Liang (2013). Analysis of Dynamic Characteristic of Sniping Rifle Barrel. *Ordnance Industry Automation* 11:30-33. (in Chinese)
- S Deng, H K Sun, C J Chiu, K C Chen (2014). Transient finite element for in-bore analysis of 9 mm pistols. *Appl Math Model* 38(9-10):2673-2688. DOI:10.1016/j.apm.2013.10.071.
- Sava A C, Piticari I L, Nistoran D G, et al (2015). The analysis of the vibratory movement of the gun barrel and its influence on the firing accuracy. *International Conference the Knowledge-based Organization* 21(3):883-887.
- Vitek R(2008). Influence of the small arm barrel bore length on the angle of jump dispersion. *Proceedings of the 7th WSEAS International Conference on System Science and Simulation in Engineering* 11: 114–118.
- Vitek R(2009). The generally unbalanced projectile load on the sporting rifle barrel. *Wseas International Conference on System Science & Simulation in Engineering* 164-169.
- Yang Yuzhao, Zhang Xiaoyun, Xu Cheng(2020a). The interaction between copper jacket projectile and barrel under different temperature based on thermo-mechanical coupling finite element model. *Journal of Vibration and Shock*, 10:44-51. (in Chinese)
- Yang Yuzhao, Zhang Xiaoyun, Xu Cheng, Fan Lixia(2020b). Dynamic stress analysis of anisotropic gun barrel under coupled thermo-mechanical loads via finite element method. *Latin American Journal of Solids and Structures* 17(1), e234.
- Zhang X, Zhu Y, Yang Y and Xu C(2019). Mechanical behaviour of lead at high strain rate. *J Mater Eng Perform* 28(10): 6268-6274.
- Zhou Ding, Xie Yushu(1999). Small parameter solution for barrel vibration caused by projectile motion in the bore. *Journal of Vibration and Shock* 18(1):76. (in Chinese)